

# BUILDING MODEL RECONSTRUCTION WITH LIDAR DATA AND TOPOGRAPHIC MAP BY REGISTRATION OF BUILDING OUTLINES

B. C. Lin<sup>1\*</sup>, R. J. You<sup>2</sup>, M. C. Hsu<sup>3</sup>

Department of Geomatics, National Cheng Kung University, 1 University Road, Tainan City, Taiwan –

<sup>1</sup>p6889102@mail.ncku.edu.tw

<sup>2</sup>rjyou@mail.ncku.edu.tw

<sup>3</sup>p66984095@mail.ncku.edu.tw

**KEY WORDS:** Tensor Voting, Feature Extraction, Registration, Robust Least Squares, Data Fusion

## ABSTRACT:

This study integrates LiDAR data and topographic map information for reconstruction of 3D building models. The procedure includes feature extraction, registration and reconstruction. In this study, the tensor voting algorithm and a region-growing method with principal features are adopted to extract building roof planes and structural lines from LiDAR data. A robust least squares method is applied to register boundary points of LiDAR data with building outlines obtained from topographic maps. The registration accuracy is about 11 cm in both x- and y- coordinates. The results of the registration method developed here are satisfactory for the subsequent application. Finally, an actual LiDAR dataset and its corresponding topographic map information demonstrate the procedure for data fusion of automatic 3D building model construction.

## 1. INTRODUCTION

The needs for building models are growing rapidly in 3D geographic information system (GIS), and hence a large number of accurate building models have become necessary to be reconstructed in a short period of time. Recent developments in airborne LiDAR have made it a new data source for 3D building model reconstruction, since LiDAR can quickly provide a large number of highly qualitative point clouds to represent building surfaces (Maas and Vosselman 1999). However, the LiDAR data has poor texture information so that the accurate building boundary extraction from LiDAR data may be difficult. Therefore, data fusion involving both LiDAR data and the existing topographic maps can improve the 3D building model reconstruction process.

A number of researchers have studied the problem of feature extraction from LiDAR data to reconstruct 3D building models (Vosselman and Dijkman 2001; Filin 2002; Overby *et al.* 2004). In general, building roof patch features are first extracted from LiDAR data. Many methods (Filin, 2002; Maas and Vosselman, 1999; Overby *et al.*, 2004) can be used for the extraction of roof patch features from LiDAR data. Next, building models are reconstructed by combining the building boundaries obtained from ground plans and intersection lines of adjacent planar faces derived from LiDAR data.

These approaches, however, may produce unreliable results in 3D building model reconstruction if the coordinate systems of LiDAR data and the ground plans are not the same. To overcome the problem of coordinate systems of various data sources, data registration is a critical step for fusion of LiDAR data and the topographic map information (Schenk and Csatho 2002; Filin *et al.* 2005; Gruen and Akca 2005; Park *et al.* 2006).

In this study, plane segments in LiDAR data are extracted in the feature space based on the tensor voting computational framework (Medioni *et al.* 2000). The tensor voting algorithm implements features such as faces, lines and points through a symmetric tensor field directly derived from data. All geometric structures (surfaces, lines and points) can therefore be inferred simultaneously. This method also offers extra information about the strength of features which can indicate the main geometric characteristic of a point.

For registration of LiDAR data and topographic maps, a robust least squares method (RLS) is adopted to estimate the transformation parameters in this study. After registration, height information and roof ridges extracted from LiDAR data are introduced to topographic maps and then the spatial positions of building outlines can be reconstructed.

In the following, the tensor voting method and the registration method are first described. Finally, an experimental result based on an actual airborne LiDAR dataset is analyzed.

## 2. FEATURE EXTRACTION

### 2.1 Tensor communication

The geometric feature of a point can be described by a second-order symmetric tensor which is expressed as follows:

$$\mathbf{T}^p = \begin{bmatrix} \bar{e}_1 & \bar{e}_2 & \bar{e}_3 \end{bmatrix} \begin{bmatrix} \lambda_1 & 0 & 0 \\ 0 & \lambda_2 & 0 \\ 0 & 0 & \lambda_3 \end{bmatrix} \begin{bmatrix} \bar{e}_1 \\ \bar{e}_2 \\ \bar{e}_3 \end{bmatrix} \quad (1)$$

\* Corresponding author.

where  $\bar{e}_1$ ,  $\bar{e}_2$  and  $\bar{e}_3$  indicate three independent and orthogonal eigenvectors;  $\lambda_1$ ,  $\lambda_2$  and  $\lambda_3$  are eigenvalues with respect to the eigenvectors  $\bar{e}_1$ ,  $\bar{e}_2$  and  $\bar{e}_3$ . The eigenvalues are real and  $\lambda_1 \geq \lambda_2 \geq \lambda_3$  if  $\mathbf{T}^p$  is a positive-semidefinite tensor. Most of LiDAR systems provide only three-dimensional Cartesian coordinates of points, and implied vector information cannot be directly obtained. The tensor voting algorithm presented here can be applied for deriving the vector information. The kernel of the tensor voting is the tensor communication among points. Each point receives vector information from its neighbouring points and stores the vector information by the tensor addition rule. The total tensor can be expressed as follows:

$$\mathbf{T} = \sum_{i=1}^m w_i \mathbf{T}_i^p \quad (2)$$

$$w(s) = \exp(-s^2 / k^2) \quad (3)$$

where  $w$  is a Gaussian decay function,  $s$  is the distance between the receiving site and the voting site, and  $k$  is a scale factor that controls the decay rate of the strength. In our experiments, the scale factor  $k$  is equal to 1.2 times the search radius, and the search radius region includes at least 20 points.

## 2.2 Tensor decomposition

After the tensor voting procedure is completed, the geometric feature information, such as planar, linear and point features, can now be detected according to the capture rules of geometric features mentioned in Medioni et al.(2000). However, the eigenvalues  $\lambda_1$ ,  $\lambda_2$  and  $\lambda_3$  are generally smaller in the border region of an object than in the central region of the same object, because the points in the border region collect fewer votes than the points in the central region do. To reduce the effect of the number of votes, the planar feature indicators  $\lambda_1 - \lambda_2$  may be normalized as

$$c_1 = \frac{(\lambda_1 - \lambda_2)}{\lambda_1} \quad (4)$$

The normalized value of planar strength are introduced for the planar feature extraction and the region growing in this study, since it is the sensitive indicator for planar features.

## 2.3 Region growing with principle feature

The region-growing method is adopted to collect the points with similar planar features. The region-growing method used here is based on the homogeneity of the principal features. The principal features of interest are the planar feature strength and the corresponding normal vectors in this study. In region-growing, only the points with the planar feature strength  $c_1$  greater than a threshold can be adopted as seed points. Since the strength of planar features in building areas is often greater than 0.96 in our experiments, the threshold is recommended to be 0.96 or larger. First, the point that has the largest  $c_1$ -value is chosen as the seed point for the planar feature extraction. A point is merged into the region if both the  $c_1$ -value and the

directional difference of the normal vector of that point are less than the corresponding thresholds. Then, the point with the second largest  $c_1$ -value in LiDAR data, excluding all extracted points in the region associated with the first seed point, is adopted as the second seed point for growing the next region. This region-growing procedure proceeds until no more seed points are available. Figure 1 illustrates segmentation result after region growing.

## 2.4 Ridge lines and boundary points

The method for extracting ridge lines used here is based on the intersection of two adjacent roof faces segmented from LiDAR data, as recommended by Maas and Vosselman (1999). The accuracy of the ridge line is about  $0.4^\circ$  in spatial angle. According to the rule that the triangles on the outer boundary of a triangular irregular network (TIN) mesh have only one or two neighboring triangles(Pu and Vosselman 2007), a TIN structure is adopted to extract boundary points.

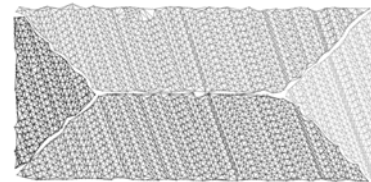


Figure 1. LiDAR points and TIN structure

## 3. FUSION OF LIDAR AND MAP

### 3.1 Registration

The first step for fusing LiDAR data and topographic map information is to transform these two datasets to a common coordinate system. The discrepancies between boundary points and building outlines are depicted in Figure 2. To determine the transformation parameters, we use robust least squares matching with the objective function which consists of the sum of squares of the distances from boundary points to building outlines on a local xy-plane.

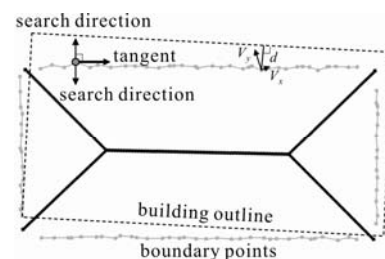


Figure 2. Boundary points and ridge lines

In order to register the boundary LiDAR points of buildings to the corresponding outline segments, a 2D similarity transformation is adopted as a mathematical tool in this study:

$$\begin{bmatrix} x' \\ y' \end{bmatrix} = \begin{bmatrix} w & u \\ -u & w \end{bmatrix} \begin{bmatrix} x \\ y \end{bmatrix} + \begin{bmatrix} r \\ s \end{bmatrix} \quad (5)$$

where  $(x,y)$  are the horizontal coordinates of a LiDAR point in a local coordinate system;  $(x',y')$  are the new coordinates in the map system after the transformation; and  $(r,s)$  are the shifts of the origin.  $w = m \cos\alpha$  and  $u = m \sin\alpha$ , where  $\alpha$  is the rotation angle and  $m$  is the scale factor.

Assume that boundary points with the new transformed coordinates should fall exactly on an outline segment represented by  $L: ax'+by'+c=0$ . By inserting Eq.(5) into the line equation  $L$ , we have the following relation:

$$(a(x+v_x)+b(y+v_y))w+(-b(x+v_x)+a(y+v_y))u+ar+bs+c=0 \quad (6)$$

where  $(a,b,c)$  can be calculated from the corresponding polygon data of an outline segment, and the residuals  $v_x$  and  $v_y$  represent two components of the distance vector from a LiDAR point to the corresponding outline segment. The RLS method developed at Stuttgart University is adopted to estimate the transformation parameters (Klein and Foerstner 1984).

The registration process is performed by iterative RLS method. In each iteration of RLS adjustment, the corresponding outline segment for each boundary LiDAR point located now by new transformed coordinates must be re-determined. The procedure proceeds until the estimated standard deviation of the distances is convergent.

### 3.2 Reconstruction

After registration, an automatic reconstruction of 3D building models is applied. In this procedure, structural lines on roofs and height information of each building outline node are needed. The height of each building node can be determined by the plane equation of a LiDAR surface segment. Structural lines are extracted by the method mentioned in section 2.4. The ridges and the building outlines are automatically connected according to following rules:

1. The structural lines derived from LiDAR data should be first extended to boundary lines on the local  $xy$ -plane, when they are shorter than they should be.
2. If the intersection point of a structural line and a boundary line is near a node point within a small region, the structural line is directly connected to the node point (case A in Figure 3).
3. If the height of a structural line at the intersection point is not different from the height of the boundary line, the structural line is directly connected to the boundary line and a new node of the boundary line is added (case B in Figure 3).
4. If the height of a structural line at the intersection point is significantly different from the height of the boundary line, two new additional structural lines may be needed (case C in Figure 3).

Then a 3D building model can be reconstructed.

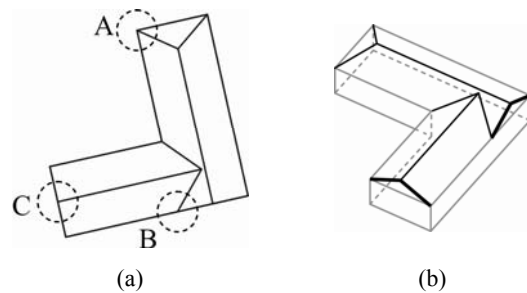


Figure 3. Connection of ridge and eave lines.

### 3.3 System overview

In summary, the proposed automatic procedure to combine data from LiDAR and topographical maps includes feature extraction, registration and reconstruction. Figure 4 illustrates this procedure. First, boundary points and ridge lines are derived from surface segments extracted from LiDAR data by the tensor voting method, and building outlines are obtained directly from corresponding 2D topographical map data. Since the coordinate systems of these two kinds of data may differ, registration of this data is necessary. Second, since it is insensitive to errors, registration of the boundary LiDAR points and the building outlines using the RLS method is recommended. Third, 3D building outlines are obtained by introducing the heights of 2D building outlines based on the plane equations of the LiDAR surface segments. Finally, the ridge lines are added and combined with the 3D building outlines for constructing building models.

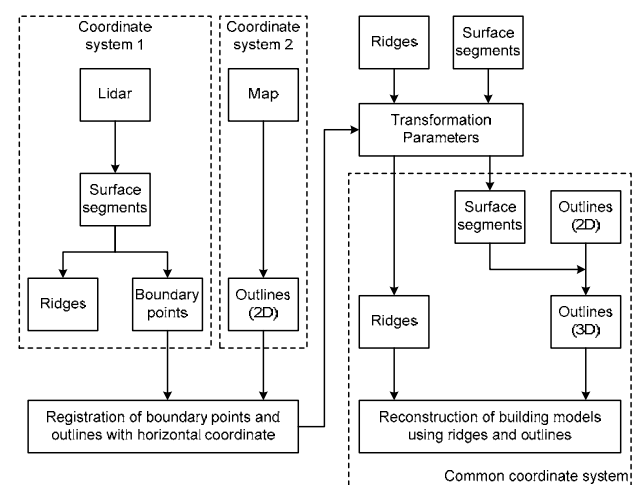


Figure 4. Procedure of automatic building model reconstruction with LiDAR data and topographic map information.

## 4. EXPERIMENT AND ANALYSIS

An airborne LiDAR dataset (LiDAR97) for an  $350 \times 500 \text{ m}^2$  experimental area was acquired by an Optech ALTM 30/70. The flying height for the laser scanning was 500 m AGL. The average LiDAR point density was  $6 \text{ pts/m}^2$ . The horizontal and vertical precision was about 25 cm and 15 cm respectively. This dataset was referred to Taiwan geodetic datum 1997.0 (TWD97). The topographic map (Map67) with scale 1:1000 for this area was produced from the aerial images and is based on Taiwan geodetic datum 1967 (TWD67). 45 building corners,

whose coordinates in both TWD67 and TWD97 were known, were selected as check points.

By comparing the registered and the known coordinates of the check points in TWD97 datum, an rms value for the coordinate differences is of about 11 cm in both x- and y- coordinates (Table 1). This indicates that the results of the registration method developed here are satisfactory for the subsequent application.

Difference	$\Delta x(m)$	$\Delta y(m)$
max	0.326	0.309
mean	0.048	-0.030
rms	0.109	0.110

Table 1. Coordinate differences of check points.

The quality of reconstructed building models is evaluated by manual check. In Figure 5, a closed polygon represents a building. Our results have shown that in total 34 of 108 buildings are incorrect building models showed with gray polygons in Figure 5 using our automatic procedure.



Figure 5. Incorrect building models (gray polygons) in the test area.

These incorrect polygons always arise on certain cases. These cases can be divided into two categories: (1) Roof faces are partly or fully covered by neighbouring buildings or trees, as shown in case A in Table 2. (2) Building outlines are not detailed enough, as shown in case B in Table 2. In cases B, small buildings are inside a big building, but the outlines of the small buildings are not drawn in the map. In all these cases, boundary LiDAR points are not sufficient to match with building outlines. This shows that these discrepancies between the boundary points and the outlines of that building influence the results of the reconstruction of building models. All of these incorrect models should be refined manually, by photogrammetry, or even field work, for instance. The complete result of automatic reconstruction of 3D building models is drawn in Figure 6.

	Actual buildings	Map + LiDAR	Reconstructed models
A			
B			

Table 2. Fusion of LiDAR data and topographic map after registration and the results of building model reconstruction.

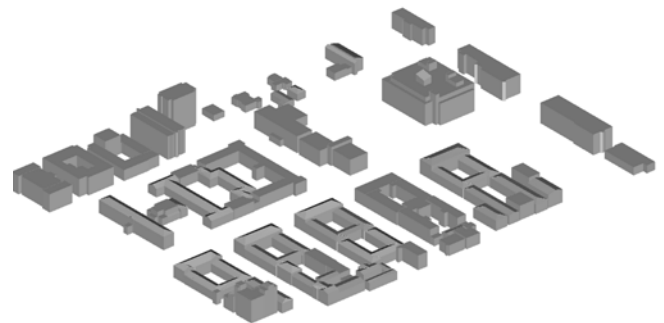


Figure 6. Complete result of automatic reconstructed building models.

## 5. CONCLUSIONS

This study has presented a novel method to construct building models by fusing LiDAR data and topographic map information. A procedure for registering the boundary points of building roof patches extracted from LiDAR data and outlines of buildings acquired from topographic maps has been proposed by a robust least squares method.

The experiments have shown that the proposed method for the building reconstruction procedure with LiDAR data and topographic map information, including feature extraction, registration and reconstruction, can be processed automatically and yields good results. Although manual editing is needed in order to achieve refined 3D building models, the results have shown that our method takes advantages of both surfaces and boundary information and improves the building reconstruction process.

## 6. REFERENCES

- Filin, S., 2002. Surface clustering from airborne laser scanning data. *International Archives of Photogrammetry and Remote Sensing*, 34(3A), pp. 119-124.
- Filin, S., Y. Kulakov and Y. Doytsher 2005. Application of Airborne Laser Technology to 3D Cadastre. *FIG Working Week 2005 and GSDI-8*, Cairo, Egypt.
- Gruen, A. and D. Akca, 2005. Least squares 3D surface and curve matching. *ISPRS Journal of Photogrammetry and Remote Sensing*, 59(3), pp. 151-174.

Klein, H. and W. Foerstner, 1984. Realization of automatic error detection in the block adjustment program PAT-M43 using robust estimators. *International Archives of Photogrammetry and Remote Sensing*, 25(A3a), pp. 234-245.

Maas, H. G. and G. Vosselman, 1999. Two algorithms for extracting building models from raw laser altimetry data. *ISPRS Journal of Photogrammetry and Remote Sensing*, 54(2-3), pp. 153-163.

Medioni, G., M. S. Lee and C. K. Tang (2000). *A computational framework for segmentation and grouping*. Elsevier Science, New York.

Overby, J., L. Bodum, E. Kjems and P. M. Ilsoe, 2004. Automatic 3D building reconstruction from airborne laser scanning and cadastral data using Hough transform. *International Archives of Photogrammetry and Remote Sensing*, 35(B3), pp. 296-302.

Park, J., I. Lee, Y. Choi and Y. J. Lee, 2006. Automatic Extraction of Large Complex Buildings Using LiDAR Data and Digital Maps. *International Archives of Photogrammetry and Remote Sensing*, 36(3), pp. 148-154.

Pu, S. and G. Vosselman, 2007. Extracting windows from terrestrial laser scanning. *International Archives of Photogrammetry Remote Sensing and Spatial Information Sciences*, 36(3/W52), pp. 320-325.

Schenk, T. and B. Csatho, 2002. Fusion of LIDAR data and aerial imagery for a more complete surface description. *International Archives of Photogrammetry and Remote Sensing*, 34(3A), pp. 310-317.

Vosselman, G. and S. Dijkman, 2001. 3D building model reconstruction from point clouds and ground plans. *International Archives of Photogrammetry and Remote Sensing*, 34(3/W4), pp. 37-43.